

AAS-PROVIDED PDF • OPEN ACCESS

How Reliable are Rotation Period Determinations from TESS Data?

To cite this article: Mariel Lares-Martiz *et al* 2024 *Res. Notes AAS* **8** 132

Manuscript version: AAS-Provided PDF

This AAS-Provided PDF is © 2024 The Author(s). Published by the American Astronomical Society.



Original content from this work may be used under the terms of the Creative Commons Attribution 4.0 licence. Any further distribution of this work must maintain attribution to the author(s) and the title of the work, journal citation and DOI.

Everyone is permitted to use all or part of the original content in this article, provided that they adhere to all the terms of the licence
<https://creativecommons.org/licenses/by/4.0>

Before using any content from this article, please refer to the Version of Record on IOPscience once published for full citation and copyright details, as permissions may be required.

View the [article online](#) for updates and enhancements.

How reliable are Rotation Period determinations from TESS data?

1 MARIEL LARES-MARTIZ ,¹ DEREK BUZASI ,² TERRY OSWALT¹ ,
2 KRYSTIAN CONFEITEIRO¹, AHNIKA GEE¹, LUCA GUIDA¹, RYAN REYNOLDS¹, and MELINDA WALLS²3 ¹*Embry-Riddle Aeronautical University*4 *1 Aerospace Blvd*5 *Daytona Beach, FL 32114, USA*6 ²*Florida Gulf Coast University*7 *10501 FGCU Blvd*8 *Fort Myers, FL 33965, USA*

9 ABSTRACT

10 Gyrochronology is the empirical relation between rotation and age. NASA's Transiting Exoplanet
11 Survey Satellite (TESS), Kepler, and K2 missions have observed thousands of wide main sequence
12 binaries. Since components of a binary are coeval, their rotation periods should be consistent with
13 gyrochronology models. However, the usefulness of gyrochronology depends upon reliable rotation
14 periods. We explore the reliability of rotation period determinations for a sample of wide binary com-
15 ponents from the TESS cycle 3. Wide binaries with the most reliable rotation period determinations
16 provide a strong basis for testing whether the gyrochronology empirical relation derived from open
17 clusters is also valid for field stars.18 *Keywords:* Rotation periods — Gyrochronology — Stellar physics — Stellar ages —

19 1. INTRODUCTION

20 Many open questions remain to be answered before gyrochronology can be established as a reliable method for
21 determining stellar ages. For example, why do old stars rotate faster than expected by Skumanich's linear prediction?
22 (Skumanich 1972), why does the period-age relation for lower main sequence stars appear to be degenerate? Further
23 studies that would like to tackle such concerns will require well-determined rotation periods for systems of the same
24 age.25 Open clusters have been the canonical systems for gyrochronology research (e.g., Barnes 2007). However, in a recent
26 study by Gruner et al. (2023), wide binary (WB) systems have shown promising results. They can be considered the
27 smallest type of open clusters, as both stars in the system share the same origin and, thus, the same age. Further,
28 both system components are separated enough to be considered equivalent to field stars with a similar wide range of
29 metallicities.30 We compiled a sample of 1956 WBs observed by TESS cycle 3 (sectors 27 to 39) for gyrochronology research purposes.
31 We create custom masks for each target using the approach outlined in Nielsen et al. (2020) and Metcalfe et al. (2023).
32 To prepare the light curves, we normalize each sector relative to its median flux and gap fill using spline interpolation.
33 We determined rotation periods for each of the 3912 components by choosing the period with the highest amplitude
34 in Lomb-Scargle periodograms (LS), the peak with the highest amplitude after $P = 0$ in auto-correlation functions
35 (ACF), and the peak with the highest relative amplitude in wavelet analyses using Morlet wavelet transform with k_0
36 = 6 (WVL). To provide a valid test of gyrochronology, it is essential to confirm that the periods detected are, in fact,
37 due to stellar rotation.38 Common challenges in ascertaining stellar rotation periods can be categorized into two primary sources: those
39 inherent to the physics of the rotation phenomenon and those related to the instrument. The first category involves
40 the ambiguity in determining the correct period when there are harmonics of the rotation period. Such situations occur
41 when there are surface spots in opposite hemispheres, (i.e., *double dippers*, Basri & Nguyen 2018) or when the angle of
42 inclination of the observation results in a non-sinusoidal shape of the light-curve (Santos et al. 2017). Likewise, a close
43 companion to the actual target results in blended light curves, which would also complicate period determinations.

44 Stellar pulsations are another source of confusion when the oscillations are in the same frequency regime as surface
 45 rotation. On the other hand, temperature changes, momentum dumps, guiding/pointing errors and downloads, among
 46 others, are the instrumental effects that may inject periodic signals into the light curve data, hampering rotation
 47 period determinations.

48 To test the reliability of our sample's rotation periods, we took two approaches: (1) comparisons to other existing
 49 rotation period pipelines and (2) examining potential instrumental periodicities to see if we mistakenly chose such a
 50 periodicity as our rotation period.

51 2. COMPARISON TO EXISTING ROTATION PERIOD PIPELINES

52 Other authors have developed complex and sophisticated pipelines to determine the surface rotation period of a
 53 large sample of stars (McQuillan et al. 2014; Santos et al. 2021; Gruner et al. 2023). These pipelines were built and
 54 tested using Kepler and K2 data. Only two stars of our sample were observed in the Kepler field. Therefore, we cannot
 55 directly compare our rotation periods with the ones determined by these pipelines. Instead, we applied our LS, ACF,
 56 and WVL algorithms to the sample studied by Gruner et al. (2023).

57 Our rotation periods from LS agreed with Gruner's in 74.4% of cases, from ACF in 60.1%, and WVL in 76.8%. We
 58 detected double Gruner's rotation period for 0.4% of the sample using LS, 2.3% when using ACF, and 0.2% when
 59 using WVL. Similarly, we detected half Gruner's rotation period for 9.4% of the sample using LS, 7.3% when using
 60 ACF, and 9.8% when using WVL.

61 In general, we found that the WVL algorithm agreed most often with the Gruner et al. (2023) periods. WVL
 62 analyses are less likely to find a harmonic of the true period. Still, LS and ACF have accurately determined the period
 63 in some situations.

64 3. INSTRUMENTAL PERIODICITIES

65 Assessing the reliability of our rotation periods involves verifying whether instrumental periodicities are causing
 66 interference. The histogram of our rotation periods displays a bimodal distribution: two peaks around 5 and 10 days.
 67 To seek the cause of this bimodality and to test for periodicities unrelated to the stellar rotation, we performed LS,
 68 ACF, and WVL analysis of our targets with the flux arrays randomized in time. The results displayed no sign of
 69 bimodality, implying that these periodicities are intrinsic to the flux data. Temperature changes and momentum
 70 dump systematics might be the origin (Vanderspek et al. 2018). These are expected to manifest as period peaks at
 71 1.5, 2, 2.5, 3, 5, and 13.7 days (Claytor et al. 2022).

72 We additionally examined the potential for minor shifts in the target centroid's x-position to contribute to contamination
 73 by computing the LS, ACF, and WVL algorithms to the x-position time series. The results are shown in Figure
 74 1, where it is evident that the periods derived from x-positions and fluxes show a strong correlation. Targets on the
 75 1:1 line (filled orange circles) confirm that some of our rotation periods are actually periodicities from a jitter-like
 76 oscillation in the x-position. A plausible explanation is that the stellar fluxes may influence the x-position. As the
 77 x-position comes from a Point Spread Function (PSF) fit to Full Frame Images (FFI) (Tenenbaum & Jenkins 2018),
 78 when the target has a close companion (i.e., Blends, which are common in TESS images, due to the large pixel size.),
 79 the PSF fit fails and seems to move toward the companion when the actual star becomes fainter (and vice versa), thus

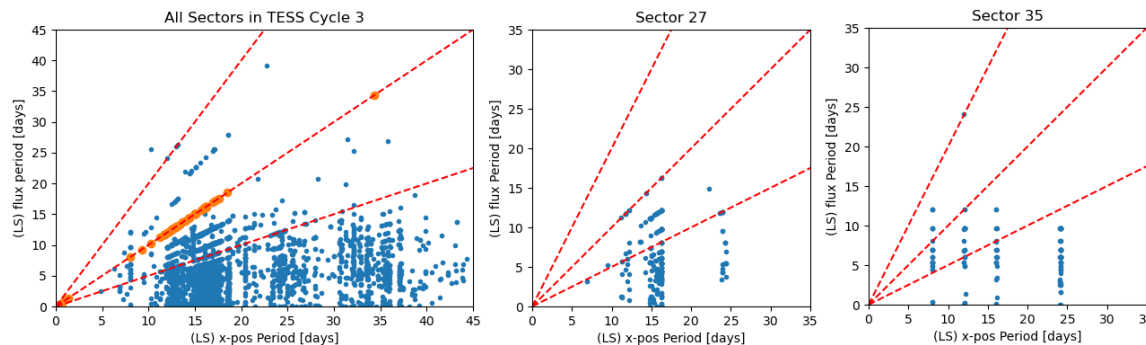


Figure 1. Comparison between detected rotation period and x-position periods. Red dashed lines mark the 2:1, 1:1, and 0.5:1 period ratios. Filled orange circles are the number of apparent rotation periods identified by the Lomb-Scargle algorithm that match periodicities found in the x-positions

80 creating a (wrongly identified) motion that directly follows the brightness changes (Gruner, private communication).
81 Moreover, the x-position movement varies by sector, as shown in the two right panels of Figure 1. The mechanisms
82 behind the distinct patterns observed within each sector remain unknown, at least to us.

83 4. CONCLUSIONS

84 So, how reliable are rotation period determinations from TESS data? To be reliable, they must be determined by
85 a dedicated pipeline tailored specifically for detecting rotation periods. Such pipelines should consider the scenarios
86 where different methods (i.e., LS, ACF, WVL) are the most reliable (see Gruner et al. 2023; Santos et al. 2021, for
87 examples of rotation period detection pipelines) and consider possible instrumental effects contaminating the data.

88 Light curve delivery from each mission involves some data preprocessing. One example is the co-trending basis vector
89 correction, wherein certain systematic trends are mitigated. The efficacy of these corrections varies, and it should be
90 noted that they are exclusively applied to flux data, not positional data. Consequently, some light curves exhibit
91 residual correlations between flux and position, while others have attenuated such correlations. Thus, relying solely on
92 periods derived from the flux data (light curves) is inadequate. A preferable approach for future work involves utilizing
93 World Coordinate System (WCS) data available in The FFI, which would enable the tracking of pixel coordinates
94 corresponding to specific celestial coordinates over time.

95 5. ACKNOWLEDGMENTS

96 Support from NSF grants AST-1910396, AST-2108975 and NASA grants 80NSSC22K0622, 80NSSC21K0245, and
97 NNX16AB76G is gratefully acknowledged. We also thank David Gruner and Zach Claytor for their valuable comments
98 and insightful contributions while interpreting certain results.

44 REFERENCES

99 Barnes, S. A. 2007, *ApJ*, 669, 1167
100 Basri, G., & Nguyen, H. T. 2018, *ApJ*, 863, 190
101 Claytor, Z. R., van Saders, J. L., Llama, J., et al. 2022,
102 *ApJ*, 927, 219
103 Gruner, D., Barnes, S. A., & Janes, K. A. 2023, *A&A*, 675,
104 A180
105 McQuillan, A., Mazeh, T., & Aigrain, S. 2014, *ApJS*, 211,
106 24
107 Metcalfe, T. S., Buzasi, D., Huber, D., et al. 2023, *AJ*, 166,
108 167
109 Nielsen, M. B., Ball, W. H., Standing, M. R., et al. 2020,
110 *A&A*, 641, A25
111 Santos, A. R. G., Breton, S. N., Mathur, S., & García,
112 R. A. 2021, *ApJS*, 255, 17
113 Santos, A. R. G., Cunha, M. S., Avelino, P. P., García,
114 R. A., & Mathur, S. 2017, *A&A*, 599, A1
115 Skumanich, A. 1972, *ApJ*, 171, 565
116 Tenenbaum, P., & Jenkins, J. M. 2018
117 Vanderspek, R., Doty, J. p., Fausnaugh, M., et al. 2018